Analysis of the Interactions in an in Situ Composite: Poly(alkylene terephthalates) Reinforced with Thermotropic Liquid Crystalline Polyesters

Gunar V. Laivins

Centre de Recherche en Sciences et Ingénierie des Macromolécules, Département de Chimie, Université Laval, Québec, Canada G1K 7P4. *Received October 5, 1988; Revised Manuscript Received March 6, 1989*

ABSTRACT: Mixtures of poly(hexamethylene terephthalate) (PHMT) and a liquid crystalline polyester of *p*-oxybenzoate and ethylene terephthalate units in a 6/4 molar ratio (LCP6/4) have morphologies that are sensitive to temperature, composition, and processing. When coprecipitated or film cast, the morphology is that of mechanical mixtures without interactions between the polymers. The amorphous phases have glass transition temperatures, T_gs, of the pure components while the crystalline phase has the same melting temperature as PHMT. Wide-angle X-ray spectra show that the lattice structures of the PHMT-LCP6/4 mixtures are those of PHMT and LCP6/4, with the structure of the major phase predominant. Differential scanning calorimetric, dynamic mechanical spectroscopic, and X-ray measurements indicate that blending at elevated temperatures creates interactions between the components. The blends exhibit a biphasic morphology where a LCP6/4 phase coexists with a semicrystalline phase. The T_g of the semicrystalline phase exceeds that of bulk PHMT and increases for blends richer in LCP6/4. The T_ms of the blends are slightly lower than that of PHMT, and the WAXS spectra indicate an altered crystal structure. NMR spectra of the extracted fraction from PHMT-LCP6/4 extrudates indicate that reactive blending has occurred. Physical processes such as dissolution could not reverse the blending that occurred at elevated temperatures. The reaction in the melt is the cause of the apparent miscibility of PHMT with LCP6/4.

Introduction

Blends where liquid crystalline polymers (LCP) reinforce thermoplastic resins from light-weight and high-strength materials. These materials combine the compressive strength of the resin with the tensile strength of the LCP fiber. The specific moduli of LCP reinforced materials may exceed the moduli of metals and conventional fiber reinforced composites.[1] LCP also facilitate the processing of the resin by lowering the melt viscosity, whereas conventional fibers and fillers thicken the melt. Furthermore the usual problems of fiber breakage and machine wear are avoided since the LCP is an ordered fluid at the processing temperature. The LCP is a processing aid when fluid and reinforces the resin when solid. Thus thermoplastic resins reinforced by thermotropic LCP blended in the melt, upon cooling spontaneously, form in situ composites.

Initially in situ composites with LCP reinforcement of the matrix required solution processing, as the LCP did not exhibit thermotropic behavior upon heating but degraded before forming an ordered fluid.[2,3] The preference for melt-processable materials that could be injection molded focused attention upon blends of thermotropic LCP with thermoplastic resins. The investigations on few systems have studied the morphology–physical property relationships[4-14] or examined the phase transitions by thermal analysis techniques.[11-23] Those morphological investigations have indicated that the blends are multiphased materials. When the LCP is the minor phase, elongated LC domains or fibrils with diameters of 1–10 μm are embedded in the resin, whereas a network structure forms at higher LCP contents. For blends where a variation in the glass transition temperatures, T_g with composition has been observed, partial miscibility has been inferred.[11-13,15-18] When blended with segmented LCP, enhanced levels of crystallinity in semi-crystalline matrix polymers with a slight depression of the melting temperature, T_m, have been reported.[13,14,16,21-23]

The objectives of this present investigation are to blend a LCP with a thermoplastic, to examine the blend for the existance of possible interactions, and to quantify the degree of interaction between the components. Specifically the mixture of poly(hexamethylene terephthalate) (PHMT) and the copolyesters of acetoxybenzoic acid (pOB) and poly(ethylene terephthalate) (PET) are examined.

A series of pOB–PET copolyesters was synthesized in the laboratories of Tennessee Eastman Kodak in 1973[24] and has been extensively studied.[25-33] The copolyesters are a family whose members have the same chemical units (pOB and PET) but have different proportions of the two groups. When heated, the members whose *p*-oxybenzoate content exceeds 38% form a nematic liquid crystalline phase.[24]

PHMT is a higher homologue of the poly(alkylene terephthalate) series. It is a semicrystalline material that melts at 155 °C and is soluble in organic solvents.[34] PHMT can be blended with the copolyester in solution or in the melt. Thus the PHMT–copolyester blends can be injection molded. With the blends, the influence of the LC copolyester on the crystal structure of PHMT can be examined. The T_g of PHMT (13 °C) and that of the copolyester (54 °C) are well separated. Thus the blend of PHMT and the pOB–PET copolyester enables a study of the variation of T_g with blend composition, while the proximity of the T_g of PET (85 °C) and PBT (43 °C) to that of LCP6/4 will obscure any variation of the T_g.

In preliminary investigations of the blends of the copolyester with PET[8,14,18,20-23,35] and with PBT,[17,36] interesting properties and morphologies have been reported. Several conclusions concerning the miscibility in these blends exist, and no specific interaction between the components has been shown. The blends of PHMT with the copolyester should be comparable to those of both PET and PBT with the copolyester, and thus the influence of the chemical structure of the resin on the properties of the blends can be analyzed.

In this investigation the blends of PHMT with the pOB–PET copolyester are analyzed by differential scanning calorimetry (DSC), dynamic mechanical spectroscopy (DMTA), proton nuclear magnetic resonance spectroscopy (NMR), and wide-angle X-ray scattering (WAXS). Evi-

0024-9297/89/2222-3974$01.50/0

dence for the apparent miscibility in the amorphous and crystalline phases is given. The interactions between PHMT and pOB–PET that render the blend miscible are elucidated. The conditions required for the interactions to occur are examined.

Experimental Section

Polymers. The weight-average molar mass of PHMT (Eastman Chemicals) in trifluoro-2-propanol measured by size exclusion chromatography is reported as 30 000 g·mol^{-1}.[34] The columns were calibrated with polystyrene standards. The T_g and T_m of the polymer had not changed from the values previously reported.[34]

The pOB–PET copolyester whose trade name is X7G was generously supplied by Tennessee Eastman Kodak. The ratio of pOB to PET units is 6/4, and the polymer is referred to as LCP6/4 in this paper. As this polymer has been the subject of numerous investigations, no further characterization is required.

Blend Preparation. The PHMT and LCP6/4 powders were combined in the ratios of 100/0, 90/10, 80/20, 70/30, 60/40, 50/50, 40/60, 30/70, 20/80, 10/90, and 0/100 to give mixtures of 0.5 g. The whole mixture was dissolved in 50 mL of 2-chlorophenol (Aldrich) at 60 °C. The polymers were coprecipitated into 500 mL of methanol, filtered, and washed several times with boiling methanol. The coprecipitated mixtures were dried at 80 °C for 3 weeks to remove the final traces of solvent in a dynamically evacuated oven.

A 0.305g mixture of PHMT and LCP6/4 powders in a 60/40 weight ratio was dissolved in 50 mL of 2-chlorophenol and a film cast. The solvent was slowly evaporated by flowing air above the solution and the film was dried until an odor could not be detected.

Samples of 1 g of each of 100/0, 80/20, 67/33, 50/50, 33/67, 20/80, and 0/100 (PHMT/LCP6/4) blends were melted at 260 °C and mixed at 100 rpm for 30–210 min in a single-screw Mini-Max Moulder CS-183 (Custom Scientific Instruments). The melt was injected into a cold mold to give uniform bars.

DSC. A Perkin-Elmer DSC-4 apparatus was used to measure the thermal transitions in the precipitated and film blends. The DSC capsule with sample was heated to 300 °C for 5–10 min, cooled to 115 °C for 15–30 min, and then quenched to −20 °C. The thermal pretreatment volatilized any entrapped solvents and avoided artifacts in the scan as the sample softened and flowed. Blends whose LCP content exceeded 30% had low crystallization temperatures. Without prior annealing, the DSC thermograms did not exhibit separate crystallization and softening phenomena. Annealing at 115 °C for 15–30 min avoided the problem by allowing the sample to crystallize. The T_g was taken at half-height in the change in the heat capacity associated with the transition. The reported T_m was the temperature that corresponded to the end of the highest temperature melting endotherm. A heating rate of 20 deg/min was used, and the thermogram was corrected for artifacts due to the variation in the base line. Every thermogram was repeated at least once more, and a duplicate blend was then analyzed to verify the reproducibility of the measurement. The thermograms of several blends were measured without any thermal pretreatment.

DMTA. A Polymer Laboratories Dynamic Mechanical Thermal Analyzer Model 2 was used to collect measurements of the PHMT and LCP6/4 samples blended at 260 °C at frequencies of 0.3, 1, and 10 Hz in the temperature interval from −10 to 110 °C. A single cantilever clamping geometry in the bending mode was used. The heating rate was 1 deg/min at a strain of ×4. The dimensions of the bar were 50 mm × 5.0 mm × 1.0 mm.

WAXS. The scattering pattern of PHMT, LCP6/4 blends precipitated from solution and the samples blended in the melt were measured in the symmetrical transmission mode with a RIGAKU Rotaflex RU200 diffractometer. The diffractometer was equipped with pinhole collimation (2-mm diameter), stepscan facilities, and a film/fiber stretching accessory. The fiber accessory enabled the sample to be rotated in a plane normal to the plane containing the incident and scattered beams (through the azimuthal angles). The sample was exposed to Ni-filtered Cu Kα radiation with an intensity of 8.0 kW emitted from the rotating anode source. The intensity of the scattered radiation was measured with a scintillation counter along the equatorial axis. The sample to receiving slit distance was 170 mm. The 2θ axis was scanned from 3° to 53° at a rate of 5 deg/min in steps of 0.1. Corrections to the scattered intensities were not applied.

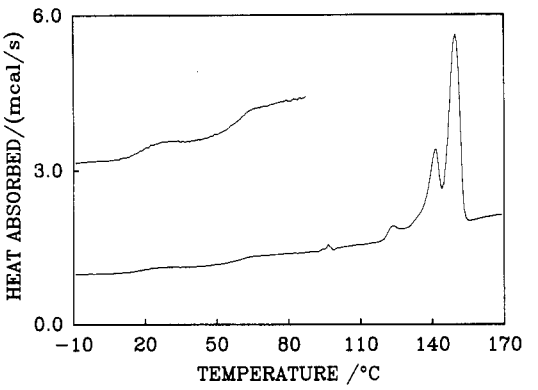

Figure 1. DSC heating thermogram of a 40PHMT–60LCP6/4 mixture that was coprecipitated into methanol from solution. The sample was heated at 300 °C for 5 min and crystallized at 115 °C for 15 min before heating at 20 deg/min when the trace was recorded. The inset (expansion of the trace) drawn to a full scale of 1.5 mcal/s indicates the two glass transitions more clearly.

NMR Spectroscopy. Samples of 50PHMT-50LCP6/4 that were blended at 260 °C for 30, 60, 90, 120, 150, and 210 min were extracted with chloroform in a Soxhlet apparatus for 24 h. The extract was rotary evaporated to dryness leaving a slightly discolored opaque film. The residue (substance contained in the thimble) was a fibrous white material.

A small quantity of the soluble material was redissolved in deuterated chloroform. The proton spectrum of the samples was measured with a Fourier transform Varian XL200 nuclear magnetic resonance spectrophotometer operating at 200 MHz.

Results and Discussion

1. Phase Transitions in PHMT–LCP6/4 Blends. The initial DSC thermogram of the pure LCP6/4 component indicates a single T_g with a midpoint at 58 ± 2 °C. In subsequent scans following equilibration at elevated temperatures, an additional broad T_g exists at 175 ± 6 °C. The existence of two T_gs for the LCP6/4 component has been attributed to the presence of blocks of both PET and pOB units in the copolymer.[17,27,28] However, a recent ^{13}C NMR study concludes that both the length and distribution of the PET and pOB sequences in the family of pOB–PET copolyesters are statistical.[25] Crystallization-induced reactions (the formation of blocks) may occur with the pOB–PET copolyesters when heated in the liquid crystal state.[37]

Prior to recording the initial heating scan, all the PHMT-LCP6/4 mixtures precipitated from solution were subjected to a thermal pretreatment. Despite the varied and complex thermal behaviors exhibited by the blends, a representative DSC heating scan for the 40PHMT–60LCP6/4 mixture is shown in Figure 1. Two T_gs and an intricate melting endotherm are present. The low-temperature T_g occurs at a temperature above that of PHMT but below that of the LCP6/4 component. The second T_g occurs at 58 °C, which is the T_g of the LCP6/4 component. The melting behavior is a mélange of several crystallization exotherms and melting endotherms. In subsequent heating scans the lower melting peak become pronounced, while the high-temperature endotherms gradually disappear. (Due to the thermal pretreatment a cold crystallization exotherm does not appear.) Complex melting phenomena are common in terephthalate polymers and are attributed to the melting of tiny imperfectly formed crystallites at low temperatures. Secondary recrystallization from the melt forms larger crystallites with a more ordered structure that melt at higher temperatures.[38]

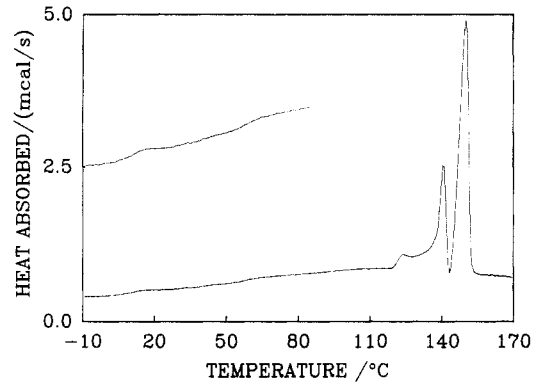

Figure 2. DSC heating thermogram of a 50PHMT–50LCP6/4 mixture that was coprecipitated into methanol from solution without any thermal pretreatment. A heating rate of 20 deg/min was used. The inset (the expansion of the trace) drawn to a full scale of 2 mcal/s indicates the two glass transitions more clearly.

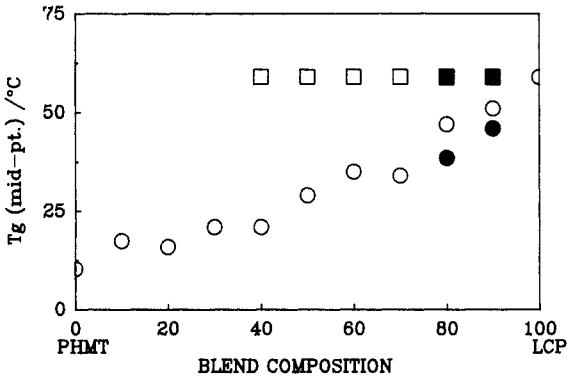

Figure 3. Variation of the glass transition temperatures of PHMT–LCP6/4 coprecipitated mixtures with blend composition: circles, lower T_g; squares, higher T_g; filled squares and filled circles, upper and lower T_g of measured T_g deconvoluted. Prior to recording the DSC traces, the mixtures were subjected to the thermal pretreatment (see text).

The initial DSC heating scan of a 50PHMT–50LCP6/4 mixture without any thermal pretreatment is shown in Figure 2. This thermogram indicates two T_gs and a melting endotherm. However, the low-temperature T_g occurs at the T_g of PHMT. The T_m is also that of PHMT and the change in the enthalpy associated with the melting phenomenon of the blend, when normalized for the PHMT content is similar to that of bulk PHMT. Thus the PHMT–LCP6/4 precipitated mixtures are mechanical blends without interactions between the components. Precipitation of the solutions into methanol apparently induces polymer segregation. The heating process established the interactions between the polymers. Thermal transitions (two T_gs and T_m) of a 60PHMT–40LCP6/4 film cast from 2-chlorophenol correspond to the transitions of the individual components. Blends of poly(butylene terephthalate) with liquid crystalline poly(biphenyl-4,4′-ylene sebacate), which are miscible in the amorphous phase, are reported to form a mechanical mixture of the components when coprecipitated in methanol from solution.[16]

The variations of glass transition temperatures with blend composition are shown in Figure 3. The low-temperature T_g is denoted by a circle and varies with blend composition. It occurs at a higher temperature than the T_g of bulk PHMT. The high-temperature T_g (square), which is the T_g of the LCP6/4 component, does not vary with blend composition. The presence of two T_gs indicates that the blends are biphasic. The change in the heat capacity of both T_gs increases as the blend becomes richer in LCP6/4. The breadth of the low-temperature T_g remains fairly constant for all the blends, which permits a deconvolution of the two T_g values for the 20/80 and 10/90 PHMT–LCP6/4 blends.

Table I
Melting Temperature and Change in Enthalpy of the Melting Endotherm for Binary PHMT–LCP6/4 Coprecipitated Blends That Had Been Thermally Conditioned

PHMT wt fractn	T_m, K	ΔH_m, cal/g	ΔH_{PHMT}, cal/g
100	428 ± 1	9.6 ± 0.2	9.6 ± 0.2
90	423 ± 1	9.75 ± 0.25	10.8 ± 0.3
80	422 ± 1	9.3 ± 0.2	11.6 ± 0.25
70	421 ± 1	7.4 ± 0.15	10.5 ± 0.2
60	422 ± 1	6.3 ± 0.1	10.5 ± 0.17
50	422.5 ± 1	5.5 ± 0.3	11.0 ± 0.6
40	420 ± 1	3.8 ± 0.2	9.6 ± 0.5
30	419 ± 1	2.8 ± 0.3	9.5 ± 1.0
20	419 ± 1	1.6 ± 0.2	7.5 ± 1.0
10	415 ± 2	0.63 ± 0.15	6.3 ± 1.5

The melting temperature, T_m, and the change in the enthalpy per gram of blend associated with the overall melting behavior, ΔH_m, and when normalized for the PHMT content, ΔH_{PHMT}, of the PHMT–LCP6/4 blends following the thermal treatment are given in Table I.

The T_m of the crystalline phase in the 90PHMT–10LCP6/4 blend is 5 °C lower than the T_m of pure PHMT. However, as the LCP6/4 content of the PHMT–LCP6/4 blends increases over the range from 90/100 to 10/90, the T_m of the crystalline phase only decreases a further 5 °C. The ΔH_m per gram of blend associated with the melting of the crystalline phase decreases for blends poorer in PHMT. When normalized for the PHMT content in the blends, the ΔH_{PHMT} value remains fairly constant. However, a significant reduction in the ΔH_{PHMT} values does occur when the PHMT content in the blends is lower than 20%.

Generally in polyblends where units of the same chemical structure in two distinct polymer cocrystallize, adjacent and dissimilar units act as impurities and deform the crystal structure.[39] Thus T_m depressions and decreasing ΔH_m values with blend composition are observed, whereas in blends of semicrystalline polymers with liquid crystalline copolyester, notably PET-LCP6/4 blends, the LCP reportedly acts as a nucleating agent for the matrix polymer.[15,20–23] Thus a higher degree of crystallinity of the matrix polymer can occur.

The dielectric and dynamic mechanical behavior of LCP6/4 copolyester with composition of 60 mol % pOB and 40 mol % PET is rather interesting, as four relaxation processes over the temperature range from −100 to 100 °C have been identified.[29–32] The relaxations on the LCP6/4 copolyester have been interpreted by a two phase model for LCP6/4: a PET-rich phase and a predominantly pOB phase.

The variations of tan δ with temperature at a frequency of 1 Hz of samples of 100/0, 67/33, 50/50, 20/80, and 0/100 (PHMT/LCP6/4), which were blended in a 260 °C melt for 45 min, are shown in Figure 4. The high-temperature relaxation mechanism ascribed to local molecular motion for the LCP6/4 component consists of a prominant peak centered at 66 °C and a relatively low intensity broad peak centered at 91 °C. The 66 °C peak is attributed to motions of PET segments hindered by interactions with pOB units, while the motions of PET units in an environment similar to the PET homopolymer occur at 91 °C.[29] A weak shoulder at 45 °C is due to relaxation of PET segments in a predominantly pOB environment. LCP6/4 also has a broad low-intensity peak spanning the temperature range from −85 to +10 °C (not shown in Figure

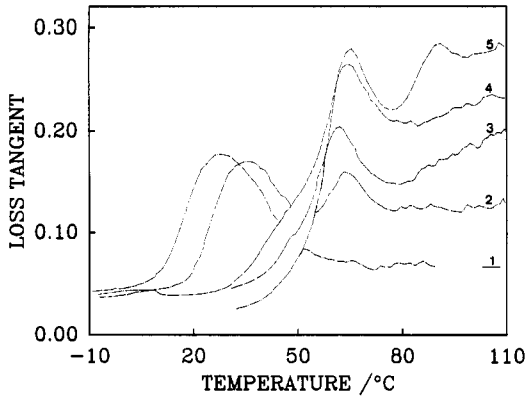

Figure 4. Variation of tan δ with temperature at a frequency of 1 Hz of extrudates of PHMT–LCP6/4 mixtures that were blended for 45 min at 260 °C. PHMT weight fractions in the extrudates are 1.0 (1), 0.67 (2), 0.50 (3), 0.20 (4), and 0.0 (5).

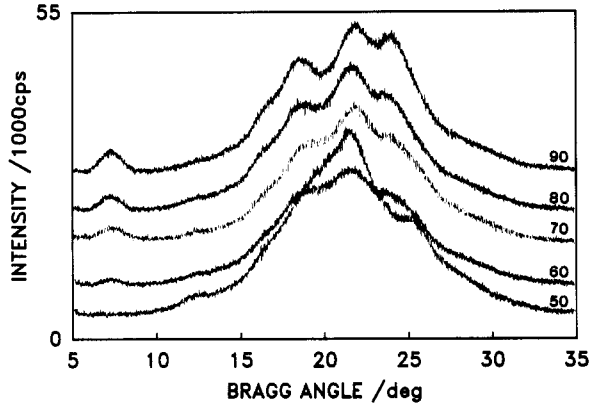

Figure 5. WAXS spectra of PHMT–LCP6/4 mixtures (coprecipitated in methanol from solution) without any thermal pretreatment. The weight fraction of PHMT in the mixture is indicated above the curve.

4). It has been ascribed to micro-Brownian motion.[14]

The tan δ relaxation spectra of the PHMT–LCP6/4 blends are characterized by several peaks. All the blends have the same broad low-intensity peak ascribed to micro-Brownian motions and a peak centered at 66 °C. However, the 91 °C peak in the relaxation spectrum of LCP6/4 is not present in the spectrum of any PHMT–LCP6/4 blend. The localized molecular motions of the PHMT units that occur at 25 °C in the homopolymer are replaced by a peak that is gradually shifted to higher temperatures as the LCP6/4 content in the blend is increased. The absence of a peak due to PHMT segments in the dynamic mechanical relaxation spectra of the extrudates indicates some type of miscibility of PHMT with LCP6/4. The blends are biphasic. A LCP6/4 phase exists in a semicrystalline matrix phase.

The wide-angle X-ray diffraction pattern of LCP6/4 is characterized by an intense but broad peak centered at a 2θ value of 20.5° with a shoulder at $\simeq$27.3° and a relatively weak broad peak at $\simeq$44°. The pOB sequences of the pOB–PET copolyesters apparently adopt the crystal structure of the parent homopolymer, poly(*p*-hydroxybenzoate).[33] The wide-angle diffraction pattern of PHMT is more interesting, with intense sharp peaks at 2θ values of 7.3°, 18.6°, 21.8°, and 24° and more diffuse peaks of low intensity at 16.6° and 42.7°.

The WAXS patterns over the Bragg angles from 5° to 35° of the 90/10, 80/20, 70/30, 60/40, and 50/50 PHMT-LCP6/4 mixtures, coprecipitated from methanol, that have not been heated are shown in Figure 5. The diffraction patterns of the mixtures whose major phase is

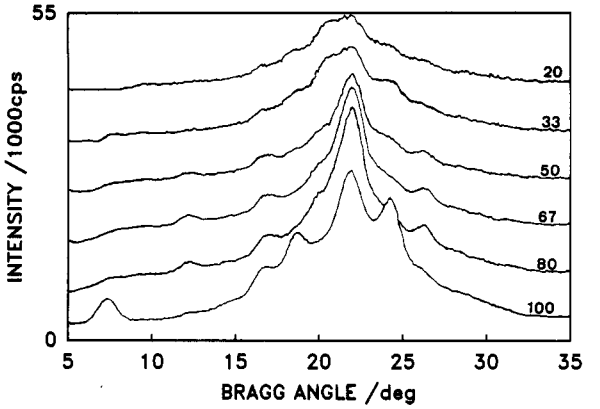

Figure 6. WAXS spectra of the non-LCP6/4 components in extrudates of PHMT–LCP6/4 mixtures blended for 45 min at 260 °C. The scattering due to the LCP6/4 component has been subtracted from the measured spectra. The weight fraction of PHMT in the mixture is indicated above the curve.

PHMT exhibit all the reflections of the PHMT component. The diffraction pattern of the 60PHMT–40LCP6/4 mixture is a broad peak with the PHMT reflections at 18.6° and 24° appearing only as ill-resolved shoulders. The mixtures whose major phase is LCP including the 50PHMT–50LCP mixture (shown in Figure 5) have diffraction patterns which resemble that of the LCP component. It appears that the presence of the LCP inhibits the crystallization of the PHMT; however, the PHMT melting endotherm at $\simeq$150 °C can be measured during a heating DSC scan. The lack of any significant variation in the 2θ positions of the PHMT reflections (i.e., no lattice deformation) and the absence of any reflection other than those in the pure components lead to the conclusion that no significant interaction occurs in the crystal phase of solution-blended mixtures.

The WAXS patterns of PHMT (lower curve) and of the 80/20, 67/33, 50/50, 33/67, and 20/80 (PHMT/LCP6/4 extrudates blended for 45 min at 260 °C without the LCP6/4 contribution are shown in Figure 6. Portion of the scattering due to the LCP6/4 component (weight fraction of powder mixed) was subtracted from the measured diffraction pattern of each extrudate to give the pattern shown. The diffraction patterns, of the crystalline phase of all the PHMT–LCP6/4 extrudates differ significantly from the diffraction pattern of PHMT crystals. Only the intense peak at 2θ of 21.8° in the spectrum of PHMT still appears in the extrudate pattern. The PHMT reflection at 16.6° becomes less intense in the patterns of the extrudates that are richer in LCP6/4. The PHMT reflections at 2θ of 7.3°, 18.6°, and 24° do not appear in the equatorial diffraction patterns of the extrudates. The WAXS patterns of the extrudates (notably those with a PHMT content >50%) have peaks centered at Bragg angles of 12.2° and 26.1°, which are not found in the diffraction pattern of unoriented PHMT. The WAXS patterns after the elimination of the LCP6/4 contribution of the 33/67 and 20PHMT/80LCP extrudates are of low intensity and thus weak peaks may not be resolved from the amorphous scattering. Clearly the crystalline phase in the extrudates has been altered by the processing conditions. It differs from the crystal structure of bulk PHMT.

The WAXS pattern of 67PHMT-33LCP6/4 extrudates blended at 260 °C for 15, 45, 100, 140, and 180 min are shown in Figure 7. The bottom curve is that of bulk PHMT. The scattering due to the LCP component has been subtracted from the measured intensities for all the extrudates except the 180-min sample. The diffraction

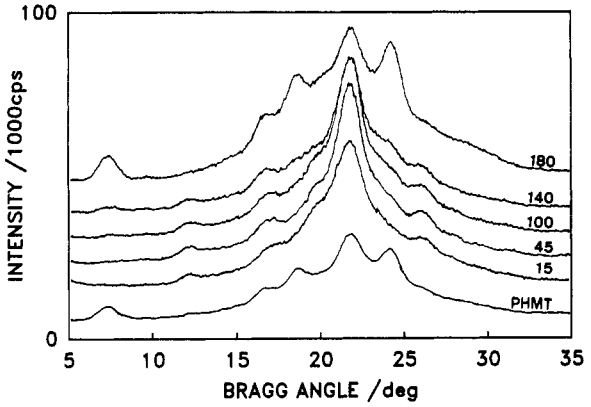

Figure 7. WAXS spectra of the non-LCP6/4 components in extrudates of a 67PHMT-33LCP6/4 mixture blended at 260 °C and of bulk PHMT. The scattering due to the LCP6/4 component has been subtracted from the measured spectra except the 180-min curve. The blending time for each mixture is indicated above the curve.

Table II
Phase Transitions in the DSC Thermograms of the Soluble Fractions Extracted with $CHCl_3$ from 50PHMT-50LCP6/4 Extrudates Blended at 260 °C

blending time, min	%[a]	T_g, K[b]	T_m, K	ΔH_m, cal g^{-1}
0	50	286 ± 2	428 ± 1	9.6 ± 0.2
30	59	298	421 ± 1	9.2 ± 0.1
60	60	300	418 ± 1	8.4 ± 0.2
90	60	300	417 ± 1	9.25 ± 0.25
120	63	301	414 ± 1	8.6 ± 0.2
150	70	298	414 ± 1	8.9 ± 0.3
210	67	302	414 ± 1	8.3 ± 0.2

[a] Percentage of the extrudate recovered in chloroform extract. [b] First scan values; on second scan the T_g values decreased.

patterns of the extrudates are similar except for the extrudate blended for 180 min. Surprisingly, the diffraction pattern of this latter extrudate is identical with the pattern of bulk PHMT, not those of the other extrudates.

The changes in the crystal structure with blending time in the extrudates at 260 °C *suggest* a reactive blending process. When blended in the melt, polycarbonate/poly(alkylene terephthalate) mixtures undergo ester interchange reactions.[40-45] Similar interchange reactions may occur in PHMT-LCP6/4 molten mixtures, and the lattice structure of the crystalline phase in the extrudates would differ from that of bulk PHMT. Changes in the equatorial reflections of the extrudates could be attributed to the injection of the melt into a mold and a subsequent preferred crystallization of PHMT. However, both the bulk PHMT and the 67PHMT-33LCP6/4 extrudate blended at 260 °C for 180 min were subject to the same processing conditions yet have similar WAXS patterns, which differ from those of the other extrudates.

2. Identification of the Specific Interaction. To investigate the nature of the interaction formed in the PHMT-LCP6/4 melt, mixtures of the components in a 1:1 weight ratio were blended for 30, 60, 90, 120, 160, and 210 min at 260 °C. The extrudates were extracted in a Soxhlet apparatus to obtain an extract and an insoluble fraction. Proton NMR spectra of the soluble extracted fraction were measured. The percentage of the extrudate recovered in the extract, transition temperatures, and enthalpy of melting of the extracted fractions are compiled in Table II.

The percentage of the extrudate recovered in the soluble fraction always exceeds the 50% of PHMT initially introduced into the mixture and the percentage grows for longer mixing times. Conversely the percentage of the extrudate recovered as insoluble residue always is less than the 50% of LCP6/4 initially introduced. Given that PHMT is soluble in hot chloroform and that LCP6/4 copolyester is insoluble in $CHCl_3$, some part of the copolyester becomes chloroform soluble.

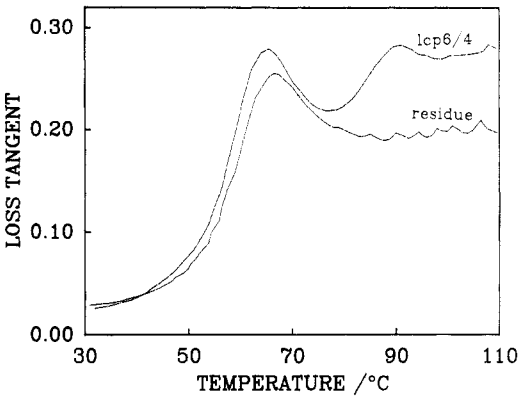

Figure 8. Variation of tan δ with temperature at a frequency of 1 Hz of extrudates of LCP6/4 and of the residue of chloroform-extracted PHMT-LCP6/4 mixtures, which were blended for 120 min at 260 °C.

Although the DSC thermogram of LCP6/4 is identical with that of the residue of extracted PHMT-LCP6/4 extrudates, some chemical modification of LCP6/4 must occur during the mixing at 260 °C (some portion of LCP6/4 became $CHCl_3$ soluble). Thus the dynamic mechanical relaxation spectrum of the residue was measured. The variations of tan δ with temperature at a frequency of 1 Hz of extrudates of LCP6/4 and of residues of extracted 50PHMT-50LCP6/4 extrudates blended for 120 min at 260 °C are shown in Figure 8. The tan δ relaxation spectra of the residue has the peak centered at 66 °C, which was attributed to motions of PET units hindered by pOB units in LCP6/4. However the 91 °C peak (relaxation of PET units in a PET environment) in the spectrum of LCP6/4 is absent in the spectrum of the residue. Evidently long PET sequences are not present in the recovered residue. This modification in the structure of LCP6/4 requires mixing with PHMT at elevated temperatures. Heating bulk LCP6/4 at 260 °C failed to produce the modification. The tan δ relaxation spectra of the PHMT-LCP6/4 extrudates do not exhibit the 91 °C peak.

The DCS thermograms of the soluble fractions indicate a single T_g and at higher temperatures a complex multipeaked endotherm similar to the melting endotherm of PHMT. The fractions that were extracted from extrudates that were blended for longer times have depressed melting temperatures and reduced change in enthalpy values. The T_gs of the soluble fraction are unremarkable except that they decrease in subsequent scans, which may indicate that rearrangement can occur when they are heated.

The proton NMR spectrum of PHMT at 200 MHz in deuterated chloroform indicates four types of absorptions. The four aromatic protons give rise to a singlet at 8.1 ppm and the four protons bonded to the ester absorb as a triplet centered at 4.4 ppm, while the eight protons located in the center of the hexamethyl sequence yield peaks at 1.6 and 1.9 ppm. The proton NMR spectra of the soluble fractions extracted from the 50PHMT-50LCP6/4 extrudates have an absorption at 4.7 ppm in addition to the absorptions of PHMT. The relative intensity (from the integration curve) of the absorption at 4.7 increases in the spectrum of the fractions that were extracted from the extrudates

that were blended for longer times. A weak absorption at 7.25 ppm in the spectrum of PHMT, which is attributed to an impurity, also appears in the spectra of the fractions. The origin of the regular increase in intensity of this peak for the extrudates is unclear.

Given that (i) the proton NMR spectra of the $CHCl_3$-soluble fraction have all the absorptions characteristic of PHMT and an additional absorption at 4.7, (ii) extraction with $CHCl_3$ of 50PHMT–50LCP6/4 extrudates blended at 260 °C shows that some part of the LCP6/4 copolyester becomes $CHCl_3$ soluble, (iii) the DSC thermogram and dynamic mechanical relaxation spectrum of the recovered insoluble residue reveal it is essentially LCP6/4 depleted of longer PET sequences, (iv) the relative abundance of the $CHCl_3$-soluble fraction and the intensity of the non-PHMT absorption (4.7 ppm) increase with the duration of the mixing at 260 °C, and (v) the absorption at 4.7 ppm corresponds to the absorption of the PET units of LCP6/4 when dissolved in trifluoroacetic acid,[25] it is thought that the longer PET sequences in LCP/4 are transferred into the PHMT phase. This assumption is supported by the fact that commercial poly(alkylene terephthalates) contain titanium residues, which have been found to catalyze transesterification reactions in blends of poly(alkylene terephthalates) with polycarbonate.[40]

With the hypothesis of the transfer of PET units from LCP6/4 to PHMT, the PHMT content in the soluble fraction would equal half of the ratio of the integration signal from the eight PHMT protons (which absorb at 1.6 and 1.9 ppm) to the *sum* of the signals of the four protons directly bonded to the ester groups from *both* the PET and PHMT (which absorb at 4.7 and 4.4, respectively). The pOB units do not absorb in these regions. The soluble fractions of the six extrudates listed in Table II have PHMT contents respectively of 75, 71, 71, 69, 71, and 68%. The PET content in the soluble fraction of the 50PHMT–50LCP6/4 would be limited to a maximum of (50)(0.4)/(20 + 50) or 0.29. In summary, the NMR spectra of the soluble fractions indicate absorptions characteristic of both PET and PHMT sequences.

The hypothesis that the interactions of PHMT with LCP6/4 developed in a reaction in the melt implies that covalent bonds are formed. In miscible blends, an electrostatic interaction between the polymers promotes segmental mixing. Miscible blends return to the initial unmixed state when the chemical environment is altered sufficiently and the physical interaction between polymers is disrupted. Conversely, upon dissolution a product of a reaction does not disassemble into the original homopolymers.

To verify that reactive blending occurred rather than the formation of a miscible blend, a 50PHMT–50LCP6/4 extrudate was blended for 30 min at 280 °C. The thermogram of the extrudate has T_gs of 33 and 58 °C, attributed to the copolymer and LCP6/4 phases, respectively. The extrudate was dissolved in 2-chlorophenol and coprecipitated in methanol. The DSC thermogram of a 50PHMT–50LCP6/4 coprecipitated mixture without any thermal pretreatment (Figure 2) indicates an absence of interactions. The dried coprecipitated extrudate without any thermal pretreatment has T_gs of 30 °C and 61 ± 2 °C. The dissolution and coprecipitation procedures could not unknit the blending that occurred at the elevated temperatures. A reaction occurs during the melt blending of PHMT-LCP6/4; miscible two component–one phase systems are not formed.

Acknowledgment. The support of the National Sciences and Engineering Council of Canada and of Université Laval is gratefully acknowledged. I thank J.-F. Croteau for the extraction experiments and D. Thibeault for the NMR spectra. Dr. G. Charlet's (Université Laval) suggestion to redissolve a heated mixture was particularly helpful.

Registry No. PHMT (SRU), 26637-42-3; PHMT (copolymer), 26618-59-7; (PHMT)($_p$OB)(PET) (copolymer), 52237-98-6.

References and Notes

(1) Takayanagi, M. *Polym. J.* **1987**, *19*, 21.
(2) Takayanagi, M.; Ogata, T.; Morikawa, M.; Kai, T. *J. Macromol. Sci., Phys. Ed.* **1980**, *B17*, 591.
(3) Helminiak, T. E. *ACS Org. Coating Plast. Prepr.* **1979**, *40*, 475. Husman, G.; Helminiak, T. E.; Adams, W.; Wiff, D.; Benner, C. L. *ACS Org. Coating Plast. Prepr.* **1979**, *40*, 797.
(4) Weiss, R. A.; Huh, W.; Nicolais, L. *Polym. Eng. Sci.* **1987**, *27*, 684.
(5) Kiss, G. *Polym. Eng. Sci.* **1987**, *27*, 410.
(6) Siegmann, A.; Dagan, A.; Kenig, S. *Polymer* **1985**, *26*, 1325.
(7) Kyu, T.; Zhuang, P. *Polym. Commun.* **1988**, *29*, 99.
(8) Nakai, A.; Shiwaku, T.; Hasegawa, H.; Hashimoto, T. *Macromolecules* **1986**, *19*, 3008.
(9) Blizard, K. G.; Baird, D. G. *Polym. Eng. Sci.* **1987**, *27*, 653.
(10) Apicella, A.; Iannelli, P.; Nicodemo, L.; Nicolais, L.; Roviello, A.; Sirigu, A. *Polym. Eng. Sci.* **1986**, *26*, 600.
(11) Jung, S. H.; Kim, S. C. *Polym. J.* **1988**, *20*, 73.
(12) Pracella, M.; Chiellini, E.; Galli, G.; Dainelli, D. *Mol. Cryst. Liq. Cryst.* **1987**, *153*, 525.
(13) Pracella, M.; Dainelli, D.; Galli, G.; Chiellini, E. *Makromol. Chem.* **1986**, *187*, 2387.
(14) Amano, M.; Nakagawa, K. *Polymer* **1987**, *28*, 263.
(15) Runt, J.; Martynowicz-Hans, L. M.; Lei, D.; Mayo, M. *ACS Polym. Prepr.* **1987**, *28*, 153.
(16) Paci, M.; Barone, C.; Magagnini, P. L. *J. Polym. Sci., Polym. Phys. Ed.*, **1987**, *25*, 1595.
(17) Kimura, M.; Porter, R. S. *J. Polym. Sci., Polym. Phys. Ed.* **1984**, *22*, 1697.
(18) Friedrich, K.; Hess, M.; Kosfeld, R. *Makromol. Chem., Macromol. Symp.* **1988**, *16*, 251.
(19) Huh, W.; Weiss, R. A.; Nicolais, L. *Proc. ACS Polym. Mat. Sci. Eng.* **1986**, *54*, 140.
(20) Joseph, E. G.; Wilkes, G. L.; Baird, D. G. *ACS Polym. Prepr.* **1983**, *24*, 304.
(21) Joseph, E. G.; Wilkes, G. L.; Baird, D. G. *Polymer Liquid Crystals* Blumstein, A., Ed.; Plenum Press: New York, 1985.
(22) Bhattacharya, S. K.; Tendolkar, A.; Misra, A. *Mol. Cryst. Liq. Cryst.* **1987**, *153*, 501.
(23) Sharma, S. K.; Tendolkar, A.; Misra, A. *Mol. Cryst. Liq. Cryst. Incl. Nonlin. Opt.* **1988**, *157*, 597.
(24) Jackson, W. J., Jr.; Kuhfuss, H. F. *J. Polym. Sci., Polym. Chem. Ed.* **1976**, *14*, 2043.
(25) Nicely, V. A.; Dougherty, J. T.; Renfro, L. W. *Macromolecules* **1987**, *20*, 573.
(26) Chiellini, E.; Lenz, R. W.; Ober, C. In *Polymer Bends*; Martuscelli, E., Palumbo, R.; Kryszewski, M., Eds.; Plenum Press: New York, 1980.
(27) Menczel, J.; Wunderlich, B. *J. Polym. Sci., Polym. Phys. Ed.* **1980**, *18*, 1433.
(28) Meesiri, W.; Menczel, J.; Gaur, U.; Wunderlich, B. *J. Polym. Sci., Polym. Phys. Ed.* **1982**, *20*, 719.
(29) Benson, R. S.; Lewis, D. N. *Polym. Commun.* **1987**, *28*, 289.
(30) Gedde, U. W., Buerger, D.; Boyd, R. H. *Macromolecules* **1987**, *20*, 988.
(31) Acierno, D.; La Mantia, F. P.; Polizzotti, G.; Ciferri, A.; Valenti, B. *Macromolecules* **1982**, *15*, 1455.
(32) Takase, Y.; Mitchell, G. R.; Odayima, A. *Polym. Commun.* **1986**, *27*, 76.
(33) Blackwell, J.; Lieser, G.; Gutierrez, G. A. *Macromolecules* **1983**, *16*, 1418.
(34) Aubin, M.; Prud'homme, R. E. *Polym. Eng. Sci.* **1984**, *24*, 350.
(35) Joseph, E.; Wilkes, G. L.; Baird, D. G. *ACS Polym. Prepr.* **1984**, *25*, 94.
(36) Desper, C. R.; Kimura, M.; Porter, R. S. *J. Polym. Sci., Polym. Phys. Ed.* **1984**, *22*, 1193.
(37) Lenz, R. W.; Jin, J.-I.; Feichtinger, K. A. *Polymer* **1983**, *24*, 327.
(38) Ponnusamy, E.; Balakrishnan, T. *Polym. J.* **1987**, *19*, 1209.
(39) Starkweather, H. W. *Polymer Compatibility and Incompatibility: Principles and Practices*; MMI Symp. Series Vol. 2; Solz, K., Ed.; Harwood Academic Press: New York, 1982.
(40) Devaux, J.; Godard, P.; Mercier, J. P. *Polym. Eng. Sci.* **1982**, *22*, 229.
(41) Devaux, J.; Godard, P.; Mercier, J. P. *J. Polym. Sci., Polym. Phys. Ed.* **1982**, *20*, 1875.

(42) Devaux, J.; Godard, P.; Mercier, J. P.; Touillaux, R.; Dereppe, J. M. J. Polym. Sci., Polym. Phys. Ed. 1982, 20, 1881.
(43) Devaux, J.; Godard, P.; Mercier, J. P. J. Polym. Sci., Polym. Phys. Ed. 1982, 20, 1895.
(44) Devaux, J.; Godard, P.; Mercier, J. P. J. Polym. Sci., Polym. Phys. Ed. 1982, 20, 1901.
(45) Pilati, F.; Marianucci, E.; Berti, C. J. Appl. Polym. Sci. 1985, 30, 1267.

Evaluation of the Lattice Strain Energy Density in Polyethylene Crystals

Hervé Marand*

Michigan Molecular Institute, 1910 W. St. Andrews Road, Midland, Michigan 48640.
Received November 16, 1988; Revised Manuscript Received March 24, 1989

ABSTRACT: Molecular energy calculations are used to assess the lattice strain energy density ϵ and the corresponding interfacial surface free energy σ_s in melt-crystallized polyethylene crystals. The quantity ϵ, which is defined as the difference in lattice energy density between an unstrained crystal and a strained crystal, is calculated with the use of published lattice expansion data. A strain-induced interfacial surface free energy σ_s of about 0.9 erg·cm^{-2} (mJ·m^{-2}) was derived from the strain energy density for a lamellar thickness of around 14 nm. This result compares favorably with the value obtained in the recent extension of nucleation theory by Hoffman and Miller describing the geometry and the growth kinetics of curved-edge polyethylene crystals.

Introduction

The goal of this paper is to provide by a direct method the value of the lattice strain energy density, which according to a recent treatment by Hoffman and Miller (HM) is at the origin of the existence of curved-edge polyethylene crystals. Hoffman and Miller proposed a generalization of the nucleation theory to account for the origin and growth kinetics of chain-folded polymer crystals with curved edges.[1] Their treatment is based on the existence of lattice strain in (200) sectors and on a detailed description of the nucleation and growth characteristics for both the (110) and the (200) sectors making the curved-edge crystal. The growth in the (110) sectors can be accounted for by standard nucleation theory,[2] where the growth front is represented by a flat surface. The growth front of the (200) sector, on the other hand, is described in the extended theory by a "serrated surface". The concomitant effect of such a serrated surface and of the lattice strain allows one to account for (1) the growth rate data obtained by Organ and Keller,[3] (2) the values of the of axial ratio and ellipticity of these curved-edge crystals,[4] and (3) the observation of different melting points for (110) and (200) sectors.[5] The agreement between theory and experiments rests, however, on the physical soundness of the value obtained for the single fitting parameter in the HM treatment, i.e., the strain-induced interfacial surface free energy σ_s, which we will calculate from the lattice strain energy density ϵ (cf. later). The parameter σ_s is involved in the kinetics of the substrate completion rate and in the expression for the reduced melting point exhibited by the (200) sectors.

The existence of lattice strain was demonstrated in the work of Davis et al.,[6] where the unit cell dimensions a and b of polyethylene crystals were measured by X-ray diffraction as a function of lamellar thickness. The steady increase of a and b dimensions with the reciprocal of lamellar thickness suggested that the lattice expansion arises from the repulsion between neighboring folds on the crystal surface. Upon careful examination of their data, it is apparent in the case of melt-crystallized polyethylene that the expansion is mainly between the (200) planes (i.e., between the (200) folds). This is consistent with the experimental observation by Bassett et al.[7] that the (200) sectors in melt-crystallized polyethylene single crystals are growth inhibited (using the concepts developed by Hoffman and Miller for the case of crystals grown from solution at low undercooling). It is also consistent with the observation of a b axis radial orientation in polyethylene spherulites. The b axis radial orientation arises from the faster growth of the (110) front as compared to the (200) (the latter is slowed down as a result of the strain between (200) planes). It can be suggested that although the growth occurs faster along the b axis, a large number of the folds will be of the (200) type, since (200) sectors occupy a much larger volume than the (110) (Figure 1). Such an hypothesis is consistent with the results of a recent study by Wittmann and Lotz.[8] Using the polymer decoration technique, they found that a large fraction of the lamellar structure had to result from lateral growth. This does not contradict the general idea that the crystallization process is kinetically controlled by nucleation on the (110) growth front. Further evidence of the repulsion between (200) planes can also be found in the recent work of Davé and Farmer,[9] where by molecular energy calculations they showed that, because of their bulkiness, (200) folds strongly repel each other.

We propose, here, to calculate the lattice strain energy density in polyethylene crystals by the technique of molecular mechanics, using the experimentally measured unit cell dimensions of Davis et al.[6]

Table I
Nonbonded Potential Parameters for C•••C, C•••H, and H•••H[a]

	A	B	C
C···C	−2.452	363 631	36.0
C···H	−0.468	32 970	36.7
H···H	−0.140	12 230	37.4

[a] A, B, and C are given respectively in J·nm^6·mol^{-1}, kJ·mol^{-1}, and nm^{-1} (from ref 14).

Molecular Mechanics

Molecular mechanics has proven very valuable in predicting the packing and structure of molecular crystals,[10,11] in providing possible mechanisms for crystal–crystal transitions,[12] in examining the energetics of chain folding,[9]

* Permanent address: Virginia Polytechnic Institute and State University, Chemistry Department, Blacksburg, Virginia 24061.

0024-9297/89/2222-3980$01.50/0